

# Quantum entanglement dynamics in a three-qubit system interacting with a spin chain

S. M. Moosavi Khansari<sup>1</sup>

*Department of Physics, Faculty of Basic Sciences, Ayatollah Boroujerdi University, Boroujerd,  
IRAN*

F. Kazemi Hasanvand

*Department of Physics, Faculty of Basic Sciences, Ayatollah Boroujerdi University, Boroujerd,  
IRAN*

In this article, we investigate the entanglement evolution of three-qubit states in the presence of a spin chain environment. Utilizing negativity as a metric for entanglement assessment, we focus on the  $GHZ$ ,  $W$ , and  $W_\xi$  quantum states as the initial system states. We explore and analyze the entanglement dynamics of these states based on various parameters.

Keywords: Entanglement dynamics, Negativity

## I Introduction

Entanglement is a key aspect of quantum mechanics that has garnered significant attention in recent years. Its applications in calculations and quantum information are noteworthy. The impossibility of completely isolating a quantum system underscores its significance. Investigating the entanglement behavior of the system's initial state in the presence of environmental effects is crucial. The interaction between the quantum system and its environment gives rise to decoherence, a phenomenon that can weaken or even terminate entanglement. This article delves into the Hamiltonian of the system-environment setup, comprising non-interacting qubits and a coupled spin chain. We explore the initial  $GHZ$  and  $W$  and  $W_\xi$  quantum states, evaluating the system environment entanglement dynamics using the negativity measure. Additionally, we examine how these dynamics vary with different parameters [1, 2, 3,4].

This study focuses on analyzing the entanglement dynamics of a qubit system within an environment. The qubits do not interact with each other but do interact with the environment, which is itself influenced by a constant magnetic field. The paper is structured as follows: Section 2 introduces the model and derives the time-dependent density. Sections 3, 4, 5, and 6 present our initial  $GHZ$  state,  $W$  state, and  $W_\xi$  state, along with their corresponding time-dependent density matrices and the measures outlined in Section 2. Finally, Section 7 contains conclusions and discussions.

---

<sup>1</sup> Email of the corresponding author: m.moosavikhansari@abru.ac.ir  
(m.moosavikhansari@gmail.com)

## II Theoretical calculations

The system comprises of three non-interacting qubits that interact with a spin chain. The total Hamiltonian is denoted as

$$H = S_A^z \sum_{k=1}^{\mathcal{N}} g^A S_{E,k}^z + S_B^z \sum_{k=1}^{\mathcal{N}} g^B S_{E,k}^z + S_C^z \sum_{k=1}^{\mathcal{N}} g^C S_{E,k}^z + \sum_{k=1}^{\mathcal{N}} h_k S_{E,k}^x \quad (1)$$

The Hamiltonian in quantum mechanics is a mathematical operator that describes the total energy of a given system. In this particular case,  $S_A^z$ ,  $S_B^z$  and  $S_C^z$  are the spin 1/2 operators in the  $z$  direction for three qubits. Meanwhile,  $S_{E,k}^z$  and  $S_{E,k}^x$  are the spin 1/2 operators in the  $z$  direction and the  $x$  direction, respectively, for the particles in the spin chain of the environment. The coupling constants of qubits  $A$ ,  $B$ , and  $C$  with this spin chain are defined as  $g^A$ ,  $g^B$  and  $g^C$ , respectively. These constants determine the strength of the interaction between the qubits and the particles in the spin chain. Moreover,  $\mathcal{N}$  denotes the number of particles in the spin chain. The Hamiltonian takes into account the interactions between the qubits and the environment, and is given by the sum of the coupling constants multiplied by the tensor products of the spin operators. Overall, these mathematical operators and constants provide a detailed description of the energy of the quantum mechanical system in question.

The initial state of the system can be seen as a three-qubit pure state represented by:

$$|\psi_s(0)\rangle = C_1|000\rangle + C_2|001\rangle + C_3|010\rangle + C_4|011\rangle + C_5|100\rangle + C_6|101\rangle + C_7|110\rangle + C_8|111\rangle \quad (2)$$

where the coefficients  $C_i$  with  $i = 1, 2, \dots, 8$  must satisfy the normalization condition:

$$\sum_{i=1}^8 |C_i|^2 = 1 \quad (3)$$

and  $|000\rangle$  represents the three-qubit system as  $|0_A\rangle \otimes |0_B\rangle \otimes |0_C\rangle$ , with the remaining states expressed similarly. We define the initial state of the environment as

$$|\psi_E(0)\rangle = \prod_{i=1}^{\mathcal{N}} (\gamma_i |0\rangle + \eta_i |1\rangle) \quad (4)$$

where the normalization condition  $|\gamma_i|^2 + |\eta_i|^2 = 1$  is required, with  $\gamma_i = \eta_i = 1/\sqrt{2}$ . We express the system's density operator, obtained by tracing out the environment, as follows:

$$\rho_s(t) = \text{tr}_E [e^{-iHt} |\psi_s(0)\rangle \langle \psi_s(0)| \otimes |\psi_E(0)\rangle \langle \psi_E(0)| e^{iHt}] \quad (5)$$

In the three-qubit computational bases  $|000\rangle, \dots, |111\rangle$ , the matrix elements  $\rho_s(t)$  are defined as follows:

$$M_{\alpha\beta} = C_\alpha C_\beta^* F_{\alpha\beta}, \quad \alpha, \beta = 1, 2, \dots, 8 \quad (6)$$

where  $F_{\alpha\beta}$ , known as decoherence factors, are defined as follows:

$$[F_{\alpha,\beta}^{\mathcal{N}}]_{\mathcal{N}=1} = (\gamma_i)^* \eta_i \left( \frac{i h_i \sin(t\Lambda_\beta) \left( \cos(t\Lambda_\alpha) + \frac{i A_\alpha \sin(t\Lambda_\alpha)}{\Lambda_\alpha} \right)}{\Lambda_\beta} - \frac{i h_i \sin(t\Lambda_\alpha) \left( \cos(t\Lambda_\beta) + \frac{i A_\beta \sin(t\Lambda_\beta)}{\Lambda_\beta} \right)}{\Lambda_\alpha} \right) + \gamma_i (\eta_i)^* \left( \frac{i h_i \sin(t\Lambda_\beta) \left( \cos(t\Lambda_\alpha) - \frac{i A_\alpha \sin(t\Lambda_\alpha)}{\Lambda_\alpha} \right)}{\Lambda_\beta} + \frac{i h_i \sin(t\Lambda_\alpha) \left( -\cos(t\Lambda_\beta) + \frac{i A_\beta \sin(t\Lambda_\beta)}{\Lambda_\beta} \right)}{\Lambda_\alpha} \right)$$

$$\begin{aligned}
& +\gamma_i(\gamma_i)^* \left( \cos(t\Lambda_\alpha) - \frac{iA_\alpha \sin(t\Lambda_\alpha)}{\Lambda_\alpha} \right) \left( \cos(t\Lambda_\beta) + \frac{iA_\beta \sin(t\Lambda_\beta)}{\Lambda_\beta} \right) \\
& +\eta_i(\eta_i)^* \left( \cos(t\Lambda_\alpha) + \frac{iA_\alpha \sin(t\Lambda_\alpha)}{\Lambda_\alpha} \right) \left( \cos(t\Lambda_\beta) - \frac{iA_\beta \sin(t\Lambda_\beta)}{\Lambda_\beta} \right) \\
& + \frac{h_i^2 \sin(t\Lambda_\alpha) \sin(t\Lambda_\beta)}{\Lambda_\alpha \Lambda_\beta}
\end{aligned} \tag{7}$$

in this mathematical relationship, the following definitions are utilized:

$$\Lambda_{\alpha(\beta)} = \sqrt{\zeta_{\alpha(\beta)}^2 + h_i^2} \tag{8}$$

$$\zeta_1 = \frac{1}{2}(g^A + g^B + g^C) \tag{9}$$

$$\zeta_2 = \frac{1}{2}(g^A + g^B - g^C) \tag{10}$$

$$\zeta_3 = \frac{1}{2}(g^A - g^B + g^C) \tag{11}$$

$$\zeta_4 = \frac{1}{2}(g^A - g^B - g^C) \tag{12}$$

$$\zeta_5 = \frac{1}{2}(-g^A + g^B + g^C) \tag{13}$$

$$\zeta_6 = \frac{1}{2}(-g^A + g^B - g^C) \tag{14}$$

$$\zeta_7 = \frac{1}{2}(-g^A - g^B + g^C) \tag{15}$$

$$\zeta_8 = \frac{1}{2}(-g^A - g^B - g^C) \tag{16}$$

We utilize the negativity measure to compute entanglement. For a quantum state with density matrix  $\rho$ , negativity is defined as follows [10]:

$$N(\rho) = \frac{\|\rho^{Tj}\| - 1}{2} \tag{17}$$

in this equation,  $\rho^{Tj}$  represents the partial transpose of the density matrix  $\rho$  concerning the  $j$  component.

### III The *GHZ* state serves as the initial state for the three-qubit system

If we consider the initial state of the system as *GHZ* state with the following relationship:

$$|\text{GHZ}\rangle = \frac{1}{\sqrt{2}}(|000\rangle + |111\rangle) \tag{18}$$

the initial density matrix of the system corresponding to this state is written as follows:

$$[\rho_s(0)]_{GHZ} = \begin{pmatrix} \frac{1}{2} & 0 & 0 & 0 & 0 & 0 & 0 & \frac{1}{2} \\ 0 & 0 & 0 & 0 & 0 & 0 & 0 & 0 \\ 0 & 0 & 0 & 0 & 0 & 0 & 0 & 0 \\ 0 & 0 & 0 & 0 & 0 & 0 & 0 & 0 \\ 0 & 0 & 0 & 0 & 0 & 0 & 0 & 0 \\ 0 & 0 & 0 & 0 & 0 & 0 & 0 & 0 \\ 0 & 0 & 0 & 0 & 0 & 0 & 0 & 0 \\ \frac{1}{2} & 0 & 0 & 0 & 0 & 0 & 0 & \frac{1}{2} \end{pmatrix} \quad (19)$$

on the other hand, the density matrix of the system in terms of the Dirac symbol after interacting with the environment is expressed as follows:

$$(\rho_s(0))_{GHZ} = \frac{1}{2}(F_{18}^*|111\rangle\langle 000| + F_{18}|000\rangle\langle 111| + |000\rangle\langle 000| + |111\rangle\langle 111|) \quad (20)$$

after some algebraic calculations, it can be rewritten as a matrix and in terms of eight bases of the corresponding three qubits as follows:

$$[\rho_s(t)]_{GHZ} = \begin{pmatrix} \frac{1}{2} & 0 & 0 & 0 & 0 & 0 & 0 & \frac{F_{18}}{2} \\ 0 & 0 & 0 & 0 & 0 & 0 & 0 & 0 \\ 0 & 0 & 0 & 0 & 0 & 0 & 0 & 0 \\ 0 & 0 & 0 & 0 & 0 & 0 & 0 & 0 \\ 0 & 0 & 0 & 0 & 0 & 0 & 0 & 0 \\ 0 & 0 & 0 & 0 & 0 & 0 & 0 & 0 \\ 0 & 0 & 0 & 0 & 0 & 0 & 0 & 0 \\ \frac{F_{18}^*}{2} & 0 & 0 & 0 & 0 & 0 & 0 & \frac{1}{2} \end{pmatrix} \quad (21)$$

First, we focus our calculations solely on the  $A$  subsystem. The partial transpose for this subsystem can be expressed as follows:

$$[\rho_s(t)]_{GHZ}^{T_A} = \begin{pmatrix} \frac{1}{2} & 0 & 0 & 0 & 0 & 0 & 0 & 0 \\ 0 & 0 & 0 & 0 & 0 & 0 & 0 & 0 \\ 0 & 0 & 0 & 0 & 0 & 0 & 0 & 0 \\ 0 & 0 & 0 & 0 & \frac{1}{2}F_{18}^* & 0 & 0 & 0 \\ 0 & 0 & 0 & \frac{1}{2}F_{18} & 0 & 0 & 0 & 0 \\ 0 & 0 & 0 & 0 & 0 & 0 & 0 & 0 \\ 0 & 0 & 0 & 0 & 0 & 0 & 0 & 0 \\ 0 & 0 & 0 & 0 & 0 & 0 & 0 & \frac{1}{2} \end{pmatrix} \quad (22)$$

Since this matrix is Hermitian, its trace norm equals the sum of the absolute values of its eigenvalues. By the negativity relation, we can express this as:

$$N_{A-BC} = \frac{1+|F_{18}|^N-1}{2} = \frac{|F_{18}|^N}{2} \quad (23)$$

Using similar calculations, we derive the following relationship for the partial transpose of the subsystem  $B$ :

$$[\rho_s(t)]_{GHZ}^{T_B} = \begin{pmatrix} \frac{1}{2} & 0 & 0 & 0 & 0 & 0 & 0 & 0 \\ 0 & 0 & 0 & 0 & 0 & 0 & 0 & 0 \\ 0 & 0 & 0 & 0 & 0 & \frac{F_{18}}{2} & 0 & 0 \\ 0 & 0 & 0 & 0 & 0 & 0 & 0 & 0 \\ 0 & 0 & 0 & 0 & 0 & 0 & 0 & 0 \\ 0 & 0 & \frac{F_{18}^*}{2} & 0 & 0 & 0 & 0 & 0 \\ 0 & 0 & 0 & 0 & 0 & 0 & 0 & 0 \\ 0 & 0 & 0 & 0 & 0 & 0 & 0 & \frac{1}{2} \end{pmatrix} \quad (24)$$

this matrix is also Hermitian, and its trace norm is equal to the sum of the absolute values of its eigenvalues. Therefore, based on the negativity relation, we can express it as:

$$N_{B-CA} = \frac{1+|F_{18}|^N-1}{2} = \frac{|F_{18}|^N}{2} \quad (25)$$

We can represent the relationship for the partial transpose of subsystem  $C$  as follows:

$$[\rho_s(t)]_{GHZ}^{T_C} = \begin{pmatrix} \frac{1}{2} & 0 & 0 & 0 & 0 & 0 & 0 & 0 \\ 0 & 0 & 0 & 0 & 0 & 0 & \frac{F_{18}}{2} & 0 \\ 0 & 0 & 0 & 0 & 0 & 0 & 0 & 0 \\ 0 & 0 & 0 & 0 & 0 & 0 & 0 & 0 \\ 0 & 0 & 0 & 0 & 0 & 0 & 0 & 0 \\ 0 & 0 & 0 & 0 & 0 & 0 & 0 & 0 \\ 0 & \frac{F_{18}^*}{2} & 0 & 0 & 0 & 0 & 0 & 0 \\ 0 & 0 & 0 & 0 & 0 & 0 & 0 & \frac{1}{2} \end{pmatrix} \quad (26)$$

it can be demonstrated that this matrix is also Hermitian and its trace norm is equal to the sum of the absolute values of its eigenvalues. Therefore, according to the negativity relation, we can express:

$$N_{C-AB} = \frac{1+|F_{18}|^N-1}{2} = \frac{|F_{18}|^N}{2} \quad (27)$$

#### IV The $W$ state serves as the initial state of the three-qubit system

Now we define the state  $W$  as the initial state of the system as follows:

$$|W\rangle = \frac{|001\rangle+|010\rangle+|100\rangle}{\sqrt{3}} \quad (28)$$

The initial density matrix of the system corresponding to this state is as follows:

$$[\rho_s(0)]_W = \begin{pmatrix} 0 & 0 & 0 & 0 & 0 & 0 & 0 & 0 \\ 0 & \frac{1}{3} & \frac{1}{3} & 0 & \frac{1}{3} & 0 & 0 & 0 \\ 0 & \frac{1}{3} & \frac{1}{3} & 0 & \frac{1}{3} & 0 & 0 & 0 \\ 0 & 0 & 0 & 0 & 0 & 0 & 0 & 0 \\ 0 & \frac{1}{3} & \frac{1}{3} & 0 & \frac{1}{3} & 0 & 0 & 0 \\ 0 & 0 & 0 & 0 & 0 & 0 & 0 & 0 \\ 0 & 0 & 0 & 0 & 0 & 0 & 0 & 0 \\ 0 & 0 & 0 & 0 & 0 & 0 & 0 & 0 \end{pmatrix} \quad (29)$$

also, the density matrix of the system in terms of the Dirac symbol after interaction with the environment for this state is calculated as follows:

$$(\rho_s(t))_W = \frac{1}{3}(F_{23}^*|010\rangle\langle 001| + F_{25}^*|100\rangle\langle 001| + F_{35}^*|100\rangle\langle 010| + F_{23}|001\rangle\langle 010| + F_{25}|001\rangle\langle 100| + F_{35}|010\rangle\langle 100| + |001\rangle\langle 001| + |010\rangle\langle 010| + |100\rangle\langle 100|) \quad (30)$$

according to the previous computation, after some algebraic calculations, it can be rewritten in the form of a matrix and in terms of eight bases of the corresponding three qubits as follows:

$$[\rho_s(t)]_W = \begin{pmatrix} 0 & 0 & 0 & 0 & 0 & 0 & 0 & 0 \\ 0 & \frac{1}{3} & \frac{F_{23}}{3} & 0 & \frac{F_{25}}{3} & 0 & 0 & 0 \\ 0 & \frac{F_{23}^*}{3} & \frac{1}{3} & 0 & \frac{F_{35}}{3} & 0 & 0 & 0 \\ 0 & 0 & 0 & 0 & 0 & 0 & 0 & 0 \\ 0 & \frac{F_{25}^*}{3} & \frac{F_{35}^*}{3} & 0 & \frac{1}{3} & 0 & 0 & 0 \\ 0 & 0 & 0 & 0 & 0 & 0 & 0 & 0 \\ 0 & 0 & 0 & 0 & 0 & 0 & 0 & 0 \\ 0 & 0 & 0 & 0 & 0 & 0 & 0 & 0 \end{pmatrix} \quad (31)$$

Based on the previous scenario, our focus is primarily on the subsystem A when performing computations. The partial transpose of this subsystem can be represented as:

$$[\rho_s(t)]_W^{T_A} = \begin{pmatrix} 0 & 0 & 0 & 0 & 0 & \frac{F_{25}^*}{3} & \frac{F_{35}^*}{3} & 0 \\ 0 & \frac{1}{3} & \frac{F_{23}}{3} & 0 & 0 & 0 & 0 & 0 \\ 0 & \frac{F_{23}^*}{3} & \frac{1}{3} & 0 & 0 & 0 & 0 & 0 \\ 0 & 0 & 0 & 0 & 0 & 0 & 0 & 0 \\ 0 & 0 & 0 & 0 & \frac{1}{3} & 0 & 0 & 0 \\ \frac{F_{25}}{3} & 0 & 0 & 0 & 0 & 0 & 0 & 0 \\ \frac{F_{35}}{3} & 0 & 0 & 0 & 0 & 0 & 0 & 0 \\ 0 & 0 & 0 & 0 & 0 & 0 & 0 & 0 \end{pmatrix} \quad (32)$$

since the matrix is Hermitian, its trace norm equals the sum of the absolute values of its eigenvalues. By the negativity relation, we can express it as:

$$N_{A-BC} = \frac{1}{3} \left( 1 + \sqrt{|F_{25}^{\mathcal{N}}|^2 + |F_{35}^{\mathcal{N}}|^2} - 1 \right) = \frac{1}{3} \sqrt{|F_{25}^{\mathcal{N}}|^2 + |F_{35}^{\mathcal{N}}|^2} \quad (33)$$

for this state, with similar calculations, we derive the following relationship for the partial transpose of the subsystem B:

$$[\rho_s(t)]_W^{T_B} = \begin{pmatrix} 0 & 0 & 0 & \frac{F_{23}^*}{3} & 0 & 0 & \frac{F_{35}}{3} & 0 \\ 0 & \frac{1}{3} & 0 & 0 & \frac{F_{25}}{3} & 0 & 0 & 0 \\ 0 & 0 & \frac{1}{3} & 0 & 0 & 0 & 0 & 0 \\ \frac{F_{23}}{3} & 0 & 0 & 0 & 0 & 0 & 0 & 0 \\ 0 & \frac{F_{25}^*}{3} & 0 & 0 & \frac{1}{3} & 0 & 0 & 0 \\ 0 & 0 & 0 & 0 & 0 & 0 & 0 & 0 \\ \frac{F_{35}^*}{3} & 0 & 0 & 0 & 0 & 0 & 0 & 0 \\ 0 & 0 & 0 & 0 & 0 & 0 & 0 & 0 \end{pmatrix} \quad (34)$$

This matrix is also Hermitian. Its trace norm is equal to the sum of the absolute values of its eigenvalues. According to the negativity relation, we can derive:

$$N_{B-CA} = \frac{1}{2} \left( 1 + \frac{2}{3} \sqrt{|F_{23}^{\mathcal{N}}|^2 + |F_{35}^{\mathcal{N}}|^2} - 1 \right) = \frac{1}{3} \sqrt{|F_{23}^{\mathcal{N}}|^2 + |F_{35}^{\mathcal{N}}|^2} \quad (35)$$

Finally, for the partial transpose of the subsystem C, the following relation can be derived:

$$[\rho_s(t)]_W^{T_C} = \begin{pmatrix} 0 & 0 & 0 & \frac{F_{23}}{3} & 0 & \frac{F_{25}}{3} & 0 & 0 \\ 0 & \frac{1}{3} & 0 & 0 & 0 & 0 & 0 & 0 \\ 0 & 0 & \frac{1}{3} & 0 & \frac{F_{35}}{3} & 0 & 0 & 0 \\ \frac{F_{23}^*}{3} & 0 & 0 & 0 & 0 & 0 & 0 & 0 \\ 0 & 0 & \frac{F_{35}^*}{3} & 0 & \frac{1}{3} & 0 & 0 & 0 \\ \frac{F_{25}^*}{3} & 0 & 0 & 0 & 0 & 0 & 0 & 0 \\ 0 & 0 & 0 & 0 & 0 & 0 & 0 & 0 \\ 0 & 0 & 0 & 0 & 0 & 0 & 0 & 0 \end{pmatrix} \quad (36)$$

This matrix is also Hermitian, and its trace norm equals the sum of the absolute values of its eigenvalues. By the negativity relation, we can express:

$$N_{C-AB} = \frac{1}{2} \left( 1 + \frac{2}{3} \sqrt{|F_{23}^{\mathcal{N}}|^2 + |F_{25}^{\mathcal{N}}|^2} - 1 \right) = \frac{1}{3} \sqrt{|F_{23}^{\mathcal{N}}|^2 + |F_{25}^{\mathcal{N}}|^2} \quad (37)$$

## V The $W_\xi$ state serves as the initial state of the three-qubit system

Finally, we define state W as the system's initial state, as follows:

$$|W_\xi\rangle = \frac{1}{\sqrt{2\xi+2}} (e^{i\delta}\sqrt{\xi+1}|001\rangle + e^{i\phi}\sqrt{\xi}|010\rangle + |100\rangle) \quad (38)$$

the initial density matrix of the system corresponding to this state is defined as follows:

$$[\rho_s(0)]_{W_\xi} = \begin{pmatrix} 0 & 0 & 0 & 0 & 0 & 0 & 0 & 0 \\ 0 & \frac{1}{2} & \frac{\xi e^{i(\delta-\phi)}}{2\sqrt{\xi(\xi+1)}} & 0 & \frac{e^{i\delta}}{2\sqrt{\xi+1}} & 0 & 0 & 0 \\ 0 & \frac{\xi e^{-i(\delta-\phi)}}{2\sqrt{\xi(\xi+1)}} & \frac{\xi}{2\xi+2} & 0 & \frac{\sqrt{\xi} e^{i\phi}}{2\xi+2} & 0 & 0 & 0 \\ 0 & 0 & 0 & 0 & 0 & 0 & 0 & 0 \\ 0 & \frac{e^{-i\delta}}{2\sqrt{\xi+1}} & \frac{\sqrt{\xi} e^{-i\phi}}{2\xi+2} & 0 & \frac{1}{2\xi+2} & 0 & 0 & 0 \\ 0 & 0 & 0 & 0 & 0 & 0 & 0 & 0 \\ 0 & 0 & 0 & 0 & 0 & 0 & 0 & 0 \\ 0 & 0 & 0 & 0 & 0 & 0 & 0 & 0 \end{pmatrix} \quad (39)$$

After performing some algebraic calculations, the density matrix of the system following interaction with the environment for this state can be expressed as a matrix and in relation to the eight bases of the corresponding three qubits as follows:

$$[\rho_s(t)]_{W_\xi} = \begin{pmatrix} 0 & 0 & 0 & 0 & 0 & 0 & 0 & 0 \\ 0 & \frac{1}{2} & \frac{F_{23}\xi e^{i(\delta-\phi)}}{2\sqrt{\xi(\xi+1)}} & 0 & \frac{e^{i\delta} F_{25}}{2\sqrt{\xi+1}} & 0 & 0 & 0 \\ 0 & \frac{\xi F_{23}^* e^{-i(\delta-\phi)}}{2\sqrt{\xi(\xi+1)}} & \frac{\xi}{2\xi+2} & 0 & \frac{F_{35}\sqrt{\xi} e^{i\phi}}{2\xi+2} & 0 & 0 & 0 \\ 0 & 0 & 0 & 0 & 0 & 0 & 0 & 0 \\ 0 & \frac{e^{-i\delta} F_{25}^*}{2\sqrt{\xi+1}} & \frac{\sqrt{\xi} e^{-i\phi} F_{35}^*}{2\xi+2} & 0 & \frac{1}{2\xi+2} & 0 & 0 & 0 \\ 0 & 0 & 0 & 0 & 0 & 0 & 0 & 0 \\ 0 & 0 & 0 & 0 & 0 & 0 & 0 & 0 \\ 0 & 0 & 0 & 0 & 0 & 0 & 0 & 0 \end{pmatrix} \quad (40)$$

In this state, we initially concentrate our calculations solely on subsystem A. For the partial transpose of this subsystem, we can express:

$$[\rho_s(t)]_{W_\xi}^{T_A} =$$



$$\begin{pmatrix}
0 & 0 & 0 & 0 & 0 & \frac{e^{-i\delta} F_{25}^*}{2\sqrt{\xi+1}} & \frac{\sqrt{\xi} e^{-i\phi} F_{35}^*}{2\xi+2} & 0 \\
0 & \frac{1}{2} & \frac{F_{23}\xi e^{i(\delta-\phi)}}{2\sqrt{\xi(\xi+1)}} & 0 & 0 & 0 & 0 & 0 \\
0 & \frac{\xi F_{23}^* e^{-i(\delta-\phi)}}{2\sqrt{\xi(\xi+1)}} & \frac{\xi}{2\xi+2} & 0 & 0 & 0 & 0 & 0 \\
0 & 0 & 0 & 0 & 0 & 0 & 0 & 0 \\
0 & 0 & 0 & 0 & \frac{1}{2\xi+2} & 0 & 0 & 0 \\
\frac{e^{i\delta} F_{25}}{2\sqrt{\xi+1}} & 0 & 0 & 0 & 0 & 0 & 0 & 0 \\
\frac{F_{35}\sqrt{\xi} e^{i\phi}}{2\xi+2} & 0 & 0 & 0 & 0 & 0 & 0 & 0 \\
0 & 0 & 0 & 0 & 0 & 0 & 0 & 0
\end{pmatrix} \quad (41)$$

Because this matrix is Hermitian, its trace norm is equal to the sum of the absolute values of the eigenvalues of this matrix. According to this point, the negativity relation can be written as follows:

$$\begin{aligned}
N_{A-BC} &= -\frac{1}{8(\xi+1)^{5/2}\sqrt{\xi(\xi+1)}} \\
&(-\xi \left| \sqrt{\xi(\xi+1)}(2\xi+1) - e^{-i(\delta+\phi)} \sqrt{e^{2i(\delta+\phi)}\xi(\xi+1)^2 (4\xi(\xi+1)|F_{23}^{\mathcal{N}}|^2 + 1)} \right| \\
&- \left| \sqrt{\xi(\xi+1)}(2\xi+1) - e^{-i(\delta+\phi)} \sqrt{e^{2i(\delta+\phi)}\xi(\xi+1)^2 (4\xi(\xi+1)|F_{23}^{\mathcal{N}}|^2 + 1)} \right| \\
&- \xi \left| \sqrt{\xi(\xi+1)}(2\xi+1) + e^{-i(\delta+\phi)} \sqrt{e^{2i(\delta+\phi)}\xi(\xi+1)^2 (4\xi(\xi+1)|F_{23}^{\mathcal{N}}|^2 + 1)} \right| \\
&- \left| \sqrt{\xi(\xi+1)}(2\xi+1) + e^{-i(\delta+\phi)} \sqrt{e^{2i(\delta+\phi)}\xi(\xi+1)^2 (4\xi(\xi+1)|F_{23}^{\mathcal{N}}|^2 + 1)} \right| \\
&- 4\sqrt{\xi(\xi+1)}(\xi+1)^{3/2} \left| \sqrt{(\xi+1)|F_{25}^{\mathcal{N}}|^2 + \xi|F_{35}^{\mathcal{N}}|^2} \right| + 4\xi\sqrt{\xi(\xi+1)}(\xi+1)^{3/2} \\
&+ 2\sqrt{\xi(\xi+1)}(\xi+1)^{3/2} \quad (42)
\end{aligned}$$

For this state, with the same calculations as before, we obtain the following relationship for the partial transpose of the subsystem  $B$ :

$$[\rho_s(t)]_{W_\xi}^{TB} =$$

$$\begin{pmatrix}
0 & 0 & 0 & \frac{\xi F_{23}^* e^{-i(\delta-\phi)}}{2\sqrt{\xi(\xi+1)}} & 0 & 0 & \frac{F_{35}\sqrt{\xi}e^{i\phi}}{2\xi+2} & 0 \\
0 & \frac{1}{2} & 0 & 0 & \frac{e^{i\delta}F_{25}}{2\sqrt{\xi+1}} & 0 & 0 & 0 \\
0 & 0 & \frac{\xi}{2\xi+2} & 0 & 0 & 0 & 0 & 0 \\
\frac{F_{23}\xi e^{i(\delta-\phi)}}{2\sqrt{\xi(\xi+1)}} & 0 & 0 & 0 & 0 & 0 & 0 & 0 \\
0 & \frac{e^{-i\delta}F_{25}^*}{2\sqrt{\xi+1}} & 0 & 0 & \frac{1}{2\xi+2} & 0 & 0 & 0 \\
0 & 0 & 0 & 0 & 0 & 0 & 0 & 0 \\
\frac{\sqrt{\xi}e^{-i\phi}F_{35}^*}{2\xi+2} & 0 & 0 & 0 & 0 & 0 & 0 & 0 \\
0 & 0 & 0 & 0 & 0 & 0 & 0 & 0
\end{pmatrix} \quad (43)$$

This matrix is also Hermitian, and its trace norm is equal to the sum of the absolute values of its eigenvalues. According to the negativity relation, we can write:

$$\begin{aligned}
N_{B-CA} &= -\frac{1}{8(\xi+1)^{5/2}\sqrt{\xi(\xi+1)}} \\
&(-\xi \left| \sqrt{\xi(\xi+1)(\xi+2)} - e^{-i(\delta+\phi)} \sqrt{e^{2i(\delta+\phi)}\xi(\xi+1)^2(\xi^2+4(\xi+1)|F_{25}^N|^2)} \right| \\
&- \left| \sqrt{\xi(\xi+1)(\xi+2)} - e^{-i(\delta+\phi)} \sqrt{e^{2i(\delta+\phi)}\xi(\xi+1)^2(\xi^2+4(\xi+1)|F_{25}^N|^2)} \right| \\
&- \xi \left| \sqrt{\xi(\xi+1)(\xi+2)} + e^{-i(\delta+\phi)} \sqrt{e^{2i(\delta+\phi)}\xi(\xi+1)^2(\xi^2+4(\xi+1)|F_{25}^N|^2)} \right| \\
&- \left| \sqrt{\xi(\xi+1)(\xi+2)} + e^{-i(\delta+\phi)} \sqrt{e^{2i(\delta+\phi)}\xi(\xi+1)^2(\xi^2+4(\xi+1)|F_{25}^N|^2)} \right| \\
&- 4\sqrt{\xi}\sqrt{\xi(\xi+1)}(\xi+1)^{3/2} \left| \sqrt{(\xi+1)|F_{23}^N|^2 + |F_{35}^N|^2} + 2\xi\sqrt{\xi(\xi+1)}(\xi+1)^{3/2} \right| \\
&+ 4\sqrt{\xi(\xi+1)}(\xi+1)^{3/2}
\end{aligned} \quad (44)$$

Finally, for the partial transpose of subsystem  $C$ , we obtain the following relationship:

$$\begin{aligned}
&[\rho_s(t)]_{W_\xi}^{T_C} = \\
&\begin{pmatrix}
0 & 0 & 0 & \frac{F_{23}\xi e^{i(\delta-\phi)}}{2\sqrt{\xi(\xi+1)}} & 0 & \frac{e^{i\delta}F_{25}}{2\sqrt{\xi+1}} & 0 & 0 \\
0 & \frac{1}{2} & 0 & 0 & 0 & 0 & 0 & 0 \\
0 & 0 & \frac{\xi}{2\xi+2} & 0 & \frac{F_{35}\sqrt{\xi}e^{i\phi}}{2\xi+2} & 0 & 0 & 0 \\
\frac{\xi F_{23}^* e^{-i(\delta-\phi)}}{2\sqrt{\xi(\xi+1)}} & 0 & 0 & 0 & 0 & 0 & 0 & 0 \\
0 & 0 & \frac{\sqrt{\xi}e^{-i\phi}F_{35}^*}{2\xi+2} & 0 & \frac{1}{2\xi+2} & 0 & 0 & 0 \\
\frac{e^{-i\delta}F_{25}^*}{2\sqrt{\xi+1}} & 0 & 0 & 0 & 0 & 0 & 0 & 0 \\
0 & 0 & 0 & 0 & 0 & 0 & 0 & 0 \\
0 & 0 & 0 & 0 & 0 & 0 & 0 & 0
\end{pmatrix} \quad (45)
\end{aligned}$$

This matrix is also Hermitian. Its trace norm equals the sum of the absolute values of its eigenvalues. Following the negativity relation, we can deduce:

$$\begin{aligned}
N_{C-AB} &= -\frac{1}{8(\xi+1)^{3/2}\sqrt{\xi(\xi+1)}} \\
&\left(-\left|\sqrt{\xi(\xi+1)^2} - e^{-i(\delta+\phi)} \sqrt{e^{2i(\delta+\phi)}\xi(\xi+1)^2 \left(4\xi|F_{35}^{\mathcal{N}}|^2 + (\xi-2)\xi+1\right)}\right|\right. \\
&\left.-\left|\sqrt{\xi(\xi+1)^2} + e^{-i(\delta+\phi)} \sqrt{e^{2i(\delta+\phi)}\xi(\xi+1)^2 \left(4\xi|F_{35}^{\mathcal{N}}|^2 + (\xi-2)\xi+1\right)}\right|\right) \\
&-4\xi\sqrt{\xi(\xi+1)}\left|\sqrt{\xi|F_{23}^{\mathcal{N}}|^2 + |F_{25}^{\mathcal{N}}|^2}\right| - 4\sqrt{\xi(\xi+1)}\left|\sqrt{\xi|F_{23}^{\mathcal{N}}|^2 + |F_{25}^{\mathcal{N}}|^2}\right| \\
&+2\sqrt{\xi(\xi+1)}(\xi+1)^{3/2}
\end{aligned} \tag{46}$$

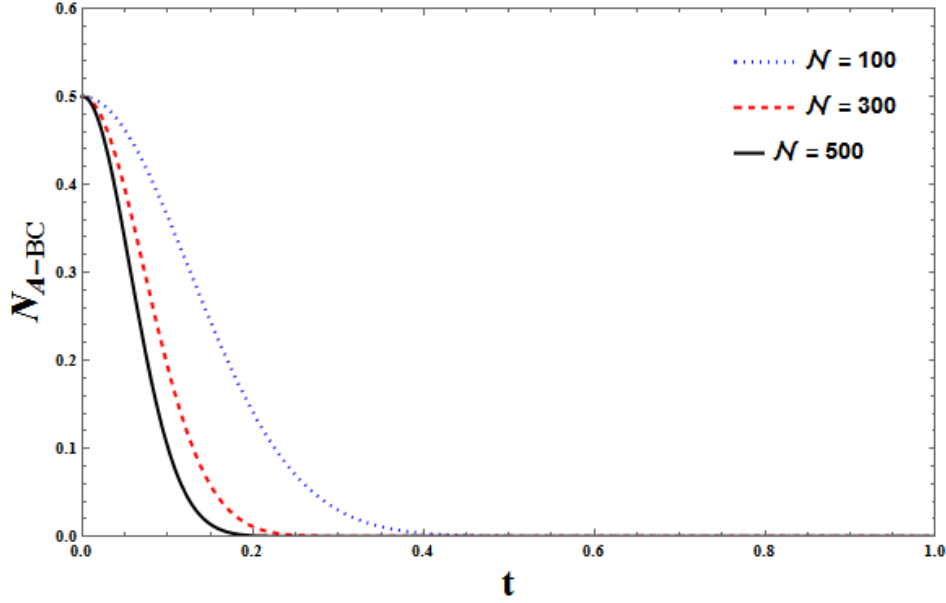


Figure 1: The negativity diagram for the *GHZ* state and the three subsystems *A*, *B*, and *C*, with specific values of  $g^A = 0.1$ ,  $g^B = 0.2$ ,  $g^C = 0.5$ ,  $h_i = 1$  and  $\gamma_i = \eta_i = 1/\sqrt{2}$ , for three varying  $\mathcal{N}$  values:  $\mathcal{N} = 100$ ,  $\mathcal{N} = 300$ ,  $\mathcal{N} = 500$ .

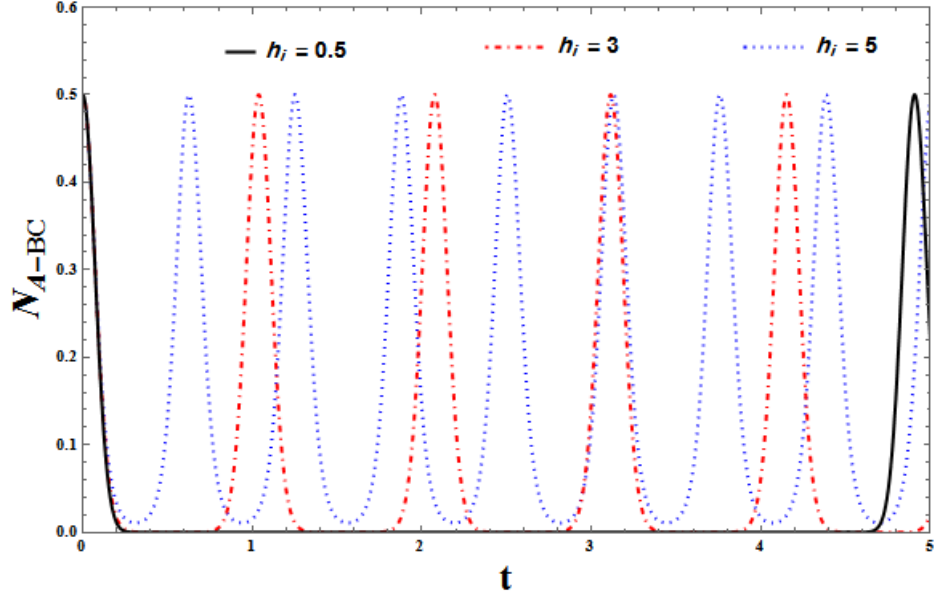


Figure 2: The negativity diagram for the *GHZ* state and the three subsystems *A*, *B*, and *C*, with given values of  $g^A = 0.1$ ,  $g^B = 0.2$ ,  $g^C = 0.5$ ,  $\mathcal{N} = 300$ , and  $\gamma_i = \eta_i = 1/\sqrt{2}$ , for three distinct values of  $h_i$ ,  $h_i = 0.5$ ,  $h_i = 3$ ,  $h_i = 5$ .

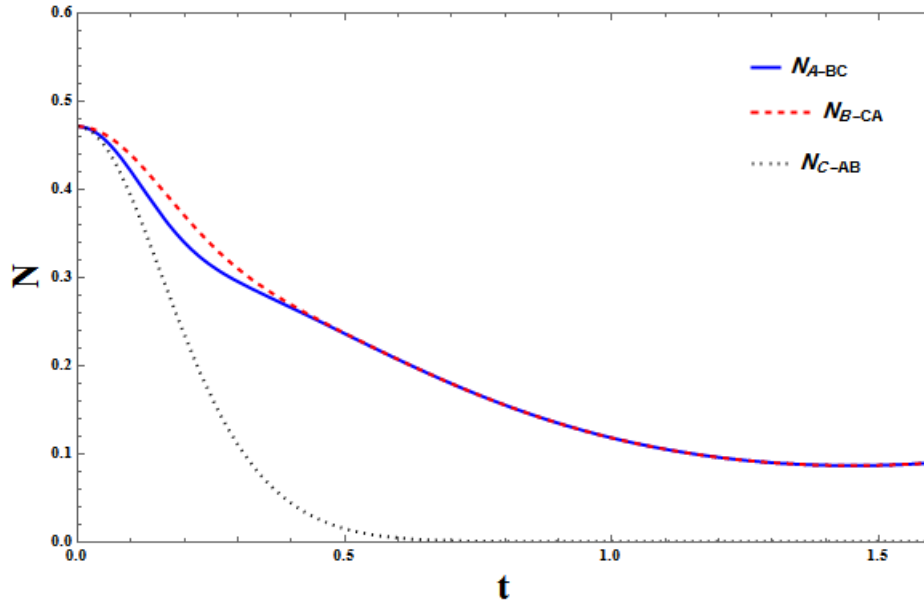


Figure 3: The negativity diagram over time for state *W* and its three corresponding subsystems *A*, *B*, and *C*. The values are as follows:  $g^A = 0.1$ ,  $g^B = 0.2$ ,  $g^C = 0.5$  and  $\mathcal{N} = 300$  and  $\gamma_i = \eta_i = 1/\sqrt{2}$  and  $h_i = 1$ .

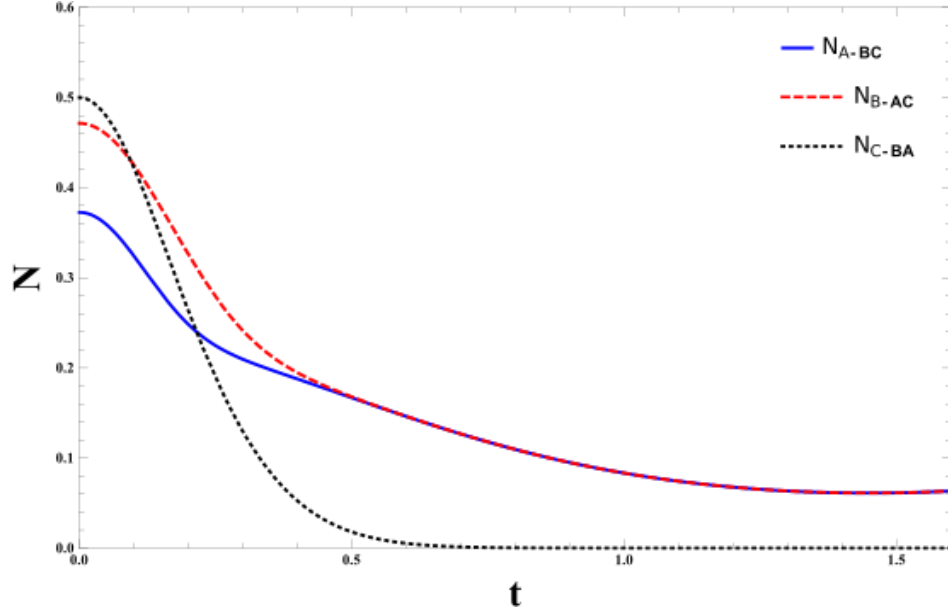


Figure 4: The time negativity diagram for state  $W_\xi$  and three subsystems  $A$ ,  $B$ , and  $C$  associated with it, with  $g^A = 0.1$ ,  $g^B = 0.2$ ,  $g^C = 0.5$  and  $\mathcal{N} = 300$ , and  $\gamma_i = \eta_i = 1/\sqrt{2}$  and  $h_i = 1$ ,  $\delta = \phi = 0$  and  $\xi = 2$ .

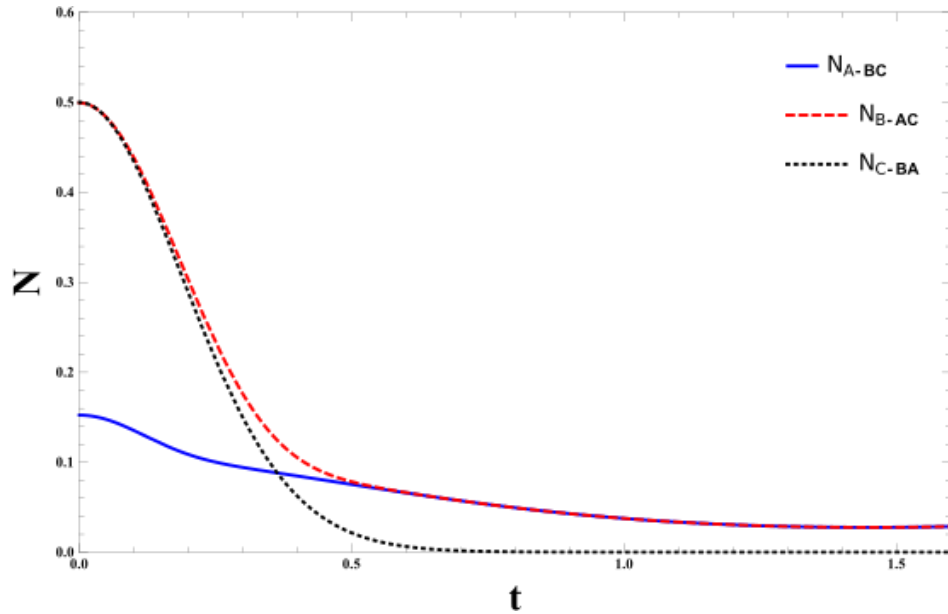


Figure 5: The time negativity diagram for the  $W_\xi$  state and its three subsystems  $A$ ,  $B$ , and  $C$ , with specific values  $g^A = 0.1$ ,  $g^B = 0.2$ ,  $g^C = 0.5$ ,  $\mathcal{N} = 300$  and  $\gamma_i = \eta_i = 1/\sqrt{2}$ . Here  $h_i = 1$ ,  $\delta = \phi = 0$  and  $\xi = 20$ .

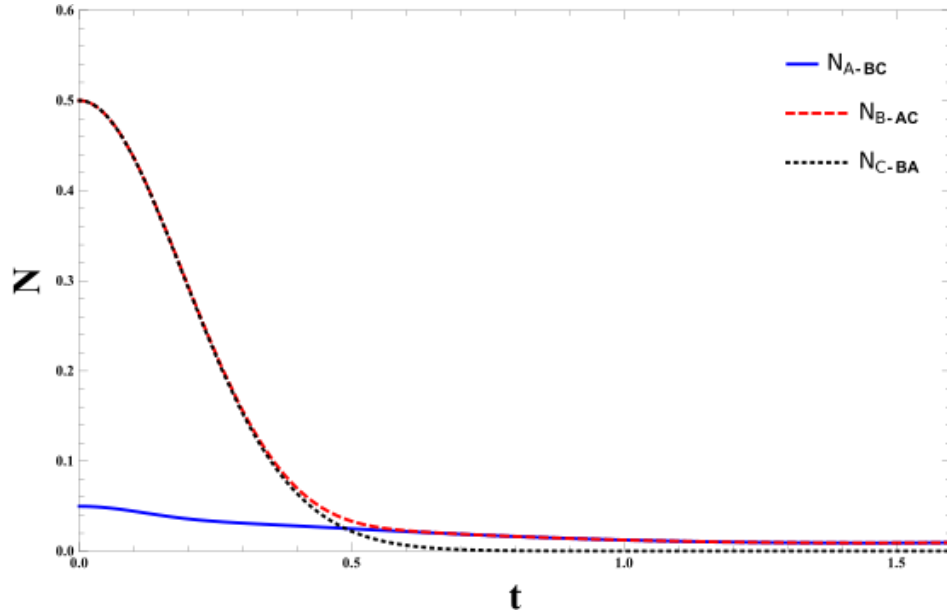


Figure 6: The time negativity diagram for the  $W_\xi$  state and its three subsystems  $A$ ,  $B$ , and  $C$ , with specific values  $g^A = 0.1$ ,  $g^B = 0.2$ ,  $g^C = 0.5$ ,  $\mathcal{N} = 300$ , and  $\gamma_i = \eta_i = 1/\sqrt{2}$ . Here  $h_i = 1$ ,  $\delta = \phi = \pi/4$  and  $\xi = 200$ .

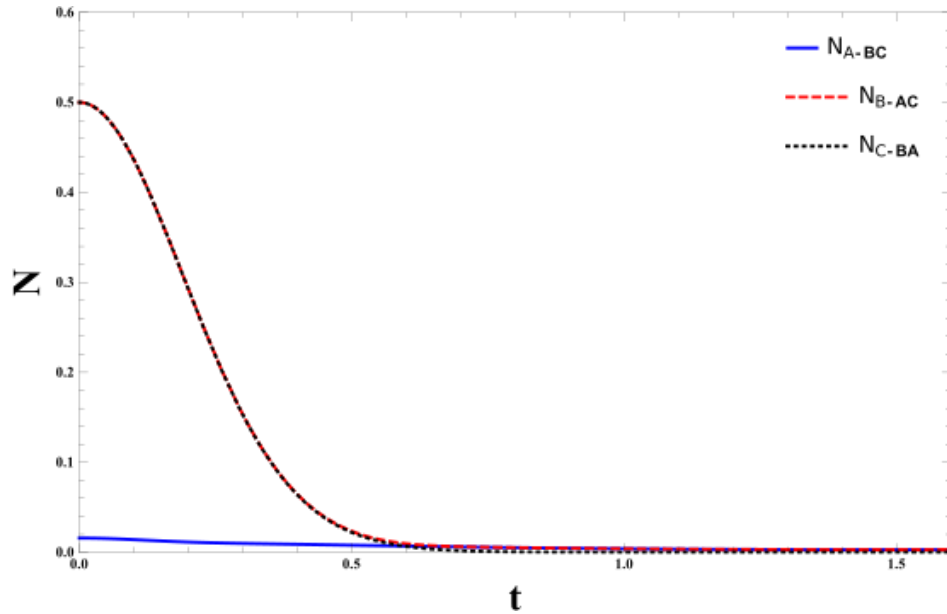


Figure 7: The time negativity diagram for the  $W_\xi$  state and its three subsystems  $A$ ,  $B$ , and  $C$ , with specific values  $g^A = 0.1$ ,  $g^B = 0.2$ ,  $g^C = 0.5$ ,  $\mathcal{N} = 300$ , and  $\gamma_i = \eta_i = 1/\sqrt{2}$ . Here  $h_i = 1$ ,  $\delta = \phi = \pi/4$  and  $\xi = 2000$ .

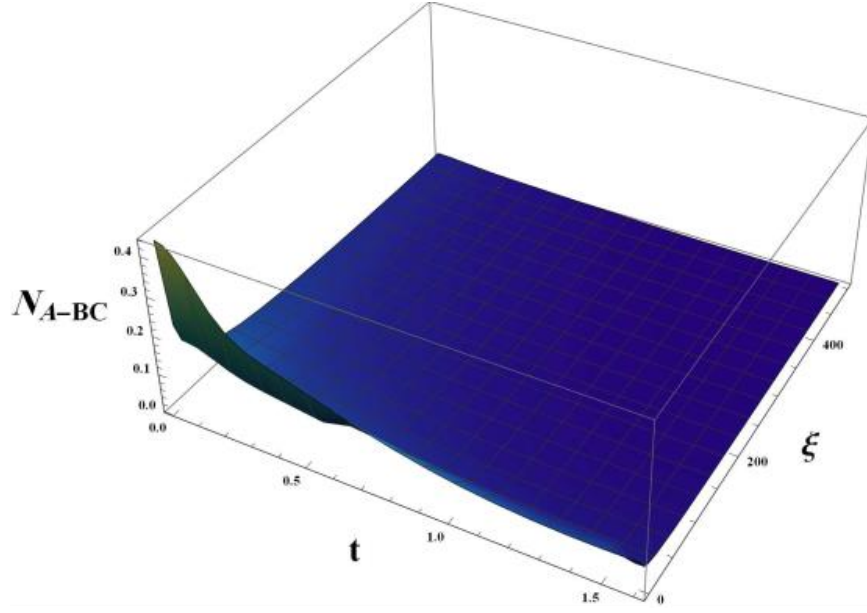


Figure 8: Graph of  $N_{A-BC}$  for state  $W_\xi$ , in terms of  $\xi$  and  $t$  for specified values of  $\delta = \phi = \pi/4$ .

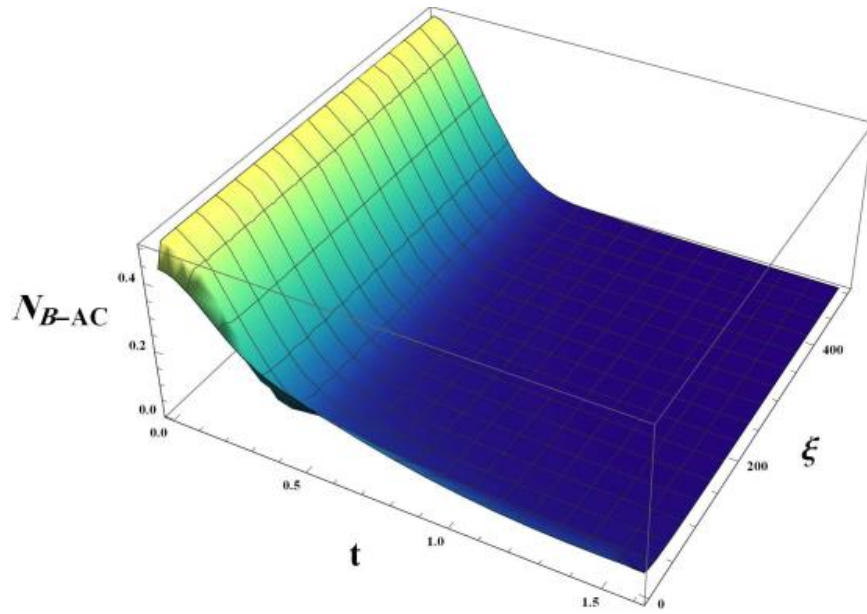


Figure 9: Graph of  $N_{B-AC}$  for state  $W_\xi$ , in terms of  $\xi$  and  $t$  for given values of  $\delta = \phi = \pi/4$ .

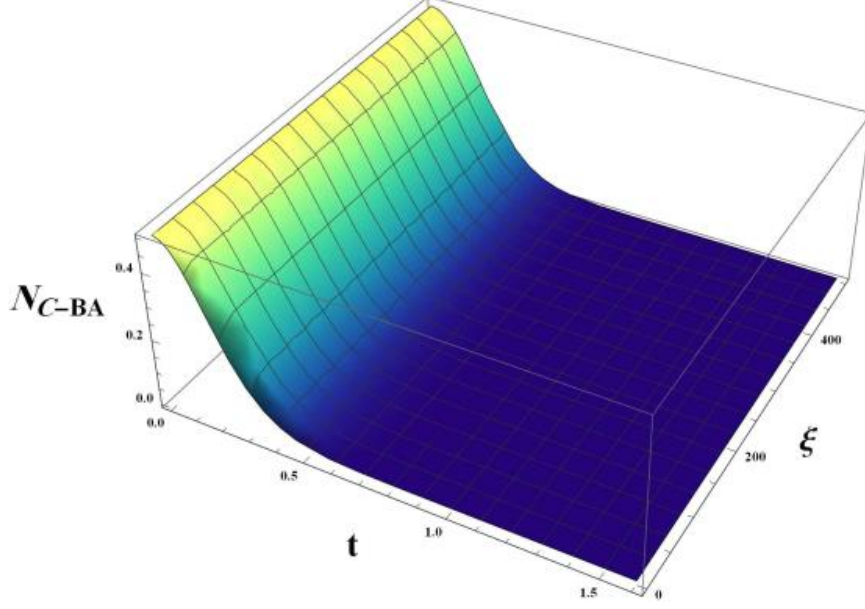


Figure 10: Graph of  $N_{C-BA}$  for state  $W_\xi$ , in terms of  $\xi$  and  $t$  for given values of  $\delta = \phi = \pi/4$ .

## VI Results and discussion

Quantum entanglement is crucial for tasks in quantum information and computation [11, 12, 13, 14, 15]. Spin systems are known for their suitability in quantum information processing, with various studies exploring their entanglement and discord properties [13, 14, 15]. However, these quantum correlations are vulnerable to decoherence caused by interactions with the environment [8, 9, 10]. While the entanglement dynamics in spin systems under decoherence from different qubit environments have been studied [5, 6, 7], the effects of decoherence from qutrit environments are yet to be explored.

We begin by presenting the results for the *GHZ* state as the initial state of the three-qubit system. Building on the topics discussed in the preceding sections, the negativity relationship remains consistent across the three subsystems  $A$ ,  $B$  and  $C$  and can be expressed as:

$$N_{A-BC} = N_{B-AC} = N_{C-AB} \quad (47)$$

Figure 1 illustrates the negativity evolution for the *GHZ* state over time with three different  $\mathcal{N}$  values. It is observed that the negativity diminishes after a certain duration; however, as the number of particles in the spin chain increases, this decay occurs more rapidly.

In Figure 2, we depict the negativity evolution for the *GHZ* state over time with three different  $h_i$  values. This figure shows that the negativity exhibits an oscillatory behavior resembling sinusoidal evolution. A higher  $h_i$  value results in a shorter period. Moreover, Figure 2 indicates that entanglement disappears at low  $h_i$  values, with the end time of entanglement extending as  $h_i$  decreases. Importantly, the negativity relationship remains consistent for the three subsystems  $A$ ,



$B$  and  $C$  in the  $GHZ$  state.

Figure 3 presents the negativity evolution over time for the  $W$  state. From this figure, it is evident that the negativity decreases over time specifically for the  $W$  state, with the loss of entanglement observed only for  $N_{C-AB}$ .

Figures 4 and 5 illustrate the time evolution of negativity for the  $W_\xi$  state with  $\delta = \phi = 0$ ,  $\xi = 2$ , and  $\xi = 20$ . Meanwhile, Figures 6 and 7 display the time evolution of negativity for the  $W_\xi$  state with  $\delta = \phi = \pi/4$ ,  $\xi = 200$  and  $\xi = 2000$ . Throughout Figures 4 to 7, it is apparent that the negativity decreases over time for the  $W_\xi$  state. As  $\xi$  increases,  $N_{B-AC}$  and  $N_{C-AB}$  converge. Consequently, in very high  $\xi$  values, entanglement ceases for these pairs. At the same time,  $N_{A-BC}$  also shows a significant reduction in entanglement for substantial  $\xi$  values.

Figures 8, 9, and 10 depict the  $N_{A-BC}$ ,  $N_{B-AC}$  and  $N_{C-AB}$  diagrams for the state  $W_\xi$  in terms of  $\xi$  and  $t$ . Overall, the analysis of Figures 8 to 10 indicates that as  $\xi$  increases over time,  $N_{B-AC}$  and  $N_{C-AB}$  remain relatively stable, whereas  $N_{A-BC}$  decreases notably with  $\xi$  growth.

The in-depth research outcomes detailed in this article show a close alignment with the data obtained from the investigations of Juo et al [16], highlighting a strong correlation between the two sets of findings.

## VII Conclusions

In this study, we explore the entanglement evolution of three-qubit states interacting with a spin chain environment. We employ negativity as a metric for evaluating entanglement. Given that negativity served as the parameter employed in the analysis of entanglement dynamics, it is plausible to regard all conceivable explications of negativity as acceptable for the dynamics of entanglement. We examined the dynamics of quantum entanglement for quantum states  $GHZ$ ,  $W$  and  $W_\xi$ , while taking into account the suggested Hamiltonian. The plots derived from our findings indicate that the negativity of the  $GHZ$  state decreases over time and decays more rapidly as the number of particles increases. The time evolution of negativity exhibits an oscillatory pattern for different  $h_i$  values. The  $W$  state also shows a decrease in negativity over time. In the  $W_\xi$  state, the negativity decreases over time, with entanglement death observed for certain subsystems as  $\xi$  increases. The analysis reveals that  $N_{B-AC}$  and  $N_{C-AB}$  remain stable, while  $N_{A-BC}$  decreases significantly as  $\xi$  increases. The research that has been carried out clearly demonstrates a significant level of alignment with the findings that have emerged from studies of a comparable nature.

## References

- [1] C. H. Bennett; "Quantum Cryptography using any two nonorthogonal states"; Phys. Rev. Lett. 28 (1992) 3121-3124. <https://doi.org/10.1103/PhysRevLett.68.3121>
- [2] C.H. Bennett, G. Brassard, C. Crepeau, et al; "Teleporting an unknown quantum state via dual classical and Einstein-Podolsky-Rosen Channels"; Phys. Rev. Lett. 70 (1993) 1895-1899. <https://doi.org/10.1103/PhysRevLett.70.1895>
- [3] C. H. Bennett and S. J. Wiesner; "Communication via one-and two-particle operators on Einstein-Podolsky-Rosen states"; Phys. Rev. Lett. 69 (1992) 2881-2884. <https://doi.org/10.1103/PhysRevLett.69.2881>
- [4] Nielsen, M. Chuang, I. (2010). Quantum Computation and Quantum Information: 10th Anniversary Edition. Cambridge: Cambridge University Press. <https://doi:10.1017/CBO9780511976667>
- [5] S. Bose;"Quantum Communication through an Unmodulated spins chain"; Phys. Rev. Lett. 91 (2003) 207901-1-4. <https://doi.org/10.1103/PhysRevLett.91.207901>
- [6] H. P. Breuer and F. Petruccione;" The Theory of open quantum systems"; Oxford University Press, Oxford, New York (2002). doi:10.1093/acprof:oso/9780199213900.001.0001
- [7] T. Yu and J.H. Eberly, "Sudden Death of Entanglement. Science 323, 598-601 (2009), doi:10.1126/science.1167343
- [8] Z. G. Yuan, P. Zhang, S. S. Li;" Disentanglement of two qubits coupled to an XY spin chain: Role of quantum phase transition"; Phys. Rev. A 76 (2007) 042118-1-7. <https://doi.org/10.1103/PhysRevA.76.042118>
- [9] Y. Y. Ying, L. Guo and T. L. Jun;" Decoherence from a spin chain with Dzyaloshinski Moriya interaction"; Chin. Phys. B. 21 (2012) 100304-1-8. doi 10.1088/1674-1056/21/10/100304
- [10] G. Vidal and R. F. Werner;"Computable measure of entanglement"; Phys. Rev. A 65 (2002) 032314. <https://doi.org/10.1103/PhysRevA.65.032314>
- [11] Timpson, C.G. 2013. Quantum Information Theory and the Foundations of Quantum Mechanics, Oxford, Oxford University Press. <https://doi.org/10.1093/acprof:oso/9780199296460.001.0001>
- [12] van Dam, W. 2013. Implausible consequences of superstrong nonlocality, Natural Computing, 12(1): 912. van Dam, W. Implausible consequences of superstrong nonlocality. Nat Comput 12, 12 (2013). <https://doi.org/10.1007/s11047-012-9353-6>
- [13] Zeilinger, A. (2018). Quantum Teleportation, Onwards and Upwards, Nature Physics, 14: 3-4. <https://doi.org/10.1038/nphys4339>
- [14] Yin, J. et al. (2017). Satellite-based Entanglement Distribution Over 1200 Kilometers, Science, 356: 11401144. doi: 10.1126/science.aan3211
- [15] Skrzypczyk, P. Brunner, N. Popescu, S. 2009. Emergence of Quantum Correlations from Nonlocality Swapping, Physical Review Letters, 102: 110402. <https://doi.org/10.1103/PhysRevLett.102.110402>
- [16] Guo, J., Song, H. Entanglement dynamics of three-qubit coupled to an XY spin chain at finite temperature with three-site interaction. Eur. Phys. J. D 61, 791-796 (2011). <https://doi.org/10.1140/epjd/e2010-10463-9>